DOI: 10.1002/anie.200903769

Medicinal Chemistry

Polyelectrolyte Microcapsules as Antigen Delivery Vehicles To Dendritic Cells: Uptake, Processing, and Cross-Presentation of Encapsulated Antigens**

Stefaan De Koker, Bruno G. De Geest, Satwinder K. Singh, Riet De Rycke, Thomas Naessens, Yvette Van Kooyk, Jo Demeester, Stefaan C. De Smedt, and Johan Grooten*

One of the major challenges for medicine today is undoubtedly the development of vaccines that can generate strong T-cell responses along with robust antibody-mediated immune responses. Induction of such strong T-cell responses is considered to be crucial to tackle insidious pathogens, such as HIV, Mycobacterium tuberculosis, and the hepatitis C virus, but also could allow an immunotherapeutic treatment of cancer.[1,2] The crucial cells in initiating T-cell responses are dendritic cells (DCs), which are specialized in internalizing antigens, processing them into small peptides, and presenting them in the cleft of their major histocompatibility complex (MHC) molecules to T cells.[3]

Exogenous foreign antigens are normally processed in endolysosomal compartments following internalization by DCs and subsequently loaded onto MHC-II molecules for presentation to CD4 T cells. In contrast, peptides derived from cytosolic proteins are loaded onto MHC-I molecules and presented to CD8 T cells. DCs also have ability to present exogenous antigens to CD8 T cells by a process called cross-presentation. For soluble antigens, this process is however extremely inefficient, and it only occurs at very high antigen doses.[4] Therefore, vaccines composed of soluble antigens largely fail to induce CD8 cytotoxic T-cell responses, which are crucial to kill virally infected cells and tumor cells.

As DCs have evolved to recognize and internalize viruses and bacteria, which are of a particulate nature, antigen encapsulation into particulates in the 0.1–10 μL range appears to be an interesting approach to achieve an improved DC targeting in vivo.[5,6] Remarkably, cross-presentation of particulate antigens occurs far more efficiently, allowing DCs to activate both CD4 and CD8 T cells in response to bacteria and viruses. Therefore, encapsulation of antigens in synthetic polymeric particles mimics the particulate nature of natural pathogens, thus enhancing antigen presentation. Enhanced cross-presentation by particulate carriers has been demonstrated for gel particles, poly(lactide-co-glycolide) microspheres, and latex particles with surface-adsorbed protein.[5,7–13] Depending on the antigen and type of carrier tested, cross-presentation occurred at 10- to 1000-fold lower doses of antigen if formulated as a particle.

Herein, we demonstrate efficient in vitro antigen delivery to DCs using polyelectrolyte capsules as microcarriers. We assess in detail how polyelectrolyte capsules are internalized by DCs as well as their intracellular fate. Using ovalbumin (OVA) as a model antigen, we demonstrate that antigen encapsulated in polyelectrolyte capsules is accessible for proteases, and is efficiently processed into peptides allowing superior presentation to both CD4 and CD8 T cells when compared to soluble antigen.

The polyelectrolyte capsules reported herein were fabricated by layer-by-layer (LbL)[14–18] coating of calcium carbonate microparticles, and co-precipitation with OVA as the sacrificial core template (Figure 1a). By mixing calcium chloride and sodium carbonate in the presence of OVA, 3 μm-sized calcium carbonate particles are formed with OVA loaded in their porous structure. After deposition of two layers of dextran sulfate/poly-L-arginine, the core templates are removed by treatment with an aqueous EDTA solution.[16,19–21] In this easy, mild and bio-friendly way, hollow capsules are obtained which are bio-compatible and degradable, both in vitro and in vivo, after uptake by phagocyting cells.[22,23]

Although polyelectrolyte microcapsule uptake by several tumor cell lines has now been reported by several groups,[24–27] the uptake mechanism is not yet fully understood.[28,29] Furthermore, the route of uptake may differ dramatically between a tumor cell line and a DC. Whilst tumor cells mainly use their increased endocytic capacity to fulfill their need for nutrients, DCs need to efficiently process the endocytosed antigens into peptides and transport them to MHC-I- and MHC-II-rich compartments to allow antigen presentation to T cells. DCs are capable of taking up microparticles by either phagocytosis or macropinocytosis. Phagocytosis is induced by ligation of specific receptors on the phagocyte surface; in

[*] Dr. B. G. De Geest
Laboratory of Pharmaceutical Technology, Department of Pharmaceutics, Ghent University (Belgium)
E-mail: br.degeest@ugent.be
Dr. S. De Koker, R. De Rycke, T. Naessens, Prof. J. Grooten
Department of Biomedical Molecular Biology, Ghent University (Belgium)
R. De Rycke
Department for Molecular Biomedical Research, VIB, Ghent (Belgium)
S. K. Singh, Prof. Y. Van Kooyk
Department of Molecular Cell Biology and Immunology, Medical Centre, Vrije Universiteit Amsterdam (The Netherlands)
Prof. J. Demeester, Prof. S. C. De Smedt
Laboratory of General Biochemistry and Physical Pharmacy, Department of Pharmaceutics, Ghent University (Belgium)

[**] B.G.D.G. thanks the FWO Vlaanderen for a postdoctoral scholarschip.

Supporting information for this article is available on the WWW under http://dx.doi.org/10.1002/anie.200903769.

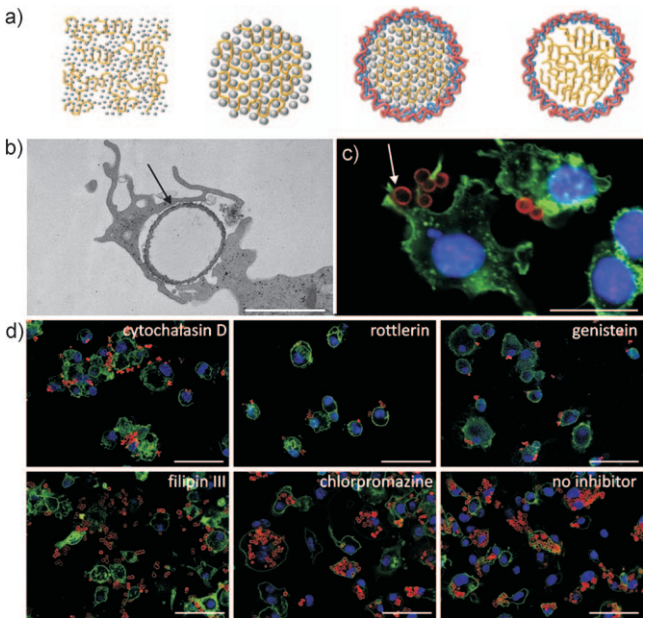

Figure 1. a) Polyelectrolyte microcapsule synthesis. A macromolecule (yellow) is mixed with $CaCl_2$ and Na_2CO_3, resulting in the generation of macromolecule-filled $CaCO_3$ microparticles (gray), which are subsequently coated with alternating layers of dextran sulfate and poly-L-arginine (red, blue). Dissolution of the $CaCO_3$ core by EDTA results in the generation of a hollow microcapsule composed of macromolecules surrounded by the polyelectrolyte shell. b,c) Images of BM-DCs taking up dextran sulfate/poly-L-arginine microcapsules. The TEM image (b) shows a BM-DC forming cytoplasmic protrusions to engulf the microcapsules (black arrow), which are visible as hollow disks with a dark, electron dense wall. Scale bar: 3 μm. c) Confocal microscopy images showing the formation of actin-rich protrusions (white arrow). The actin cytoskelet was stained with alexa 488 phalloidin (green). Microcapsules were labeled red by incorporation of RITC–poly-L-arginine. Nuclei were stained blue with Hoechst 33258. Scale bar: 10 μm. d) Confocal images of the effects of cytochalasin D (10 $\mu g\,mL^{-1}$), rottlerin (25 $\mu g\,mL^{-1}$), genistein (50 $\mu g\,mL^{-1}$), filipin III (10 $\mu g\,mL^{-1}$), and chlorpromazine (10 $\mu g\,mL^{-1}$) on microcapsule uptake by BM-DCs. Scale bars: 50 μm.

contrast, macropinocytosis is receptor-independent and initiated by membrane ruffling. These membrane ruffles then fuse and form large intracellular vesicles (0.2–10 μm) containing extracellular fluid. Though the underlying mechanisms are still largely unclear, the route of antigen internalization strongly affects the way the antigen is processed and presented to T cells.[30,31]

Figure 1 b,c shows images of capsules internalized by DCs, which were obtained from the bone marrow of mice. From the observed formation of actin-rich plasma membrane extensions, a macropinocytotic uptake route is proposed. These observations were further confirmed using a set of uptake inhibitors (Figure 1 d). Microcapsule uptake was inhibited by cytochalasin D, an inhibitor of actin polymerization that is known to block both phagocytosis and macropinocytosis, and blocked by incubation with rottlerin, a recently identified selective inhibitor of macropinocytosis.[32] Remarkably, both genistein and filipin III,[33,34] two known inhibitors of caveolae-mediated endocytosis, but not chlorpromazine,[35] an inhibitor of the clathrin pathway of endocytosis, inhibited microcapsule internalization. Caveolae-mediated uptake of polyelectrolyte microcapsules by tumor cells has been described recently,[21] indicating DCs and tumor cells might internalize polyelectrolyte microcapsules by similar mechanisms.

Once internalized by DCs, polyelectrolyte microcapsules appear to end up in acidic compartments, as demonstrated by the co-localization of rhodamine-labeled microcapsules (red fluorescence) with Lysotracker Green (green), resulting in a yellow color due to overlap (Figure 2 a). No co-localization was observed after cytoplasmic staining with CellTracker Green (green fluorescence). These results are in agreement with those obtained by Parak et al.,[29] who were able to trace polyelectrolyte microcapsules to acidic compartments following uptake by tumor cell lines by encapsulating the pH-sensitive dye SNARF-1. In contrast, we observed at least a partial co-localization (Manders' coefficient of 0.49 ± 0.11) with the lysosomal marker Lamp-1 after a 24 h incubation period (Figure 2 a, white arrows).

Although deformation of polyelectrolyte microcapsules following cellular uptake has been reported,[36] it remained unclear whether the wall of the microcapsules is ruptured and whether they are able to escape from the acidic compartments and release their content into the cytoplasm,[37] or remain confined to endolysosomal structures.[38] Using transmission

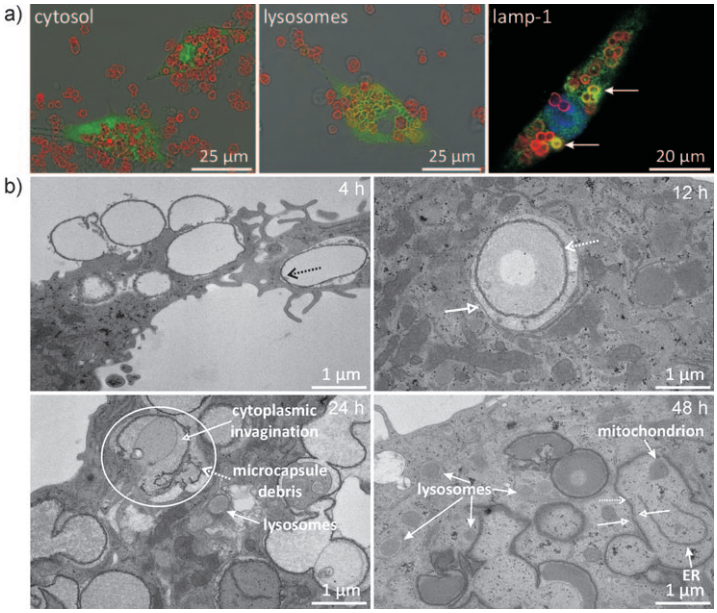

Figure 2. a) Confocal images of BM-DCs incubated with dextran sulfate/poly-L-arginine microcapsules for 24 h. The shell of the microcapsules was labeled red by incorporation of RITC-poly-L-arginine. DCs were stained with CellTracker Green (left panel) to visualize the cytoplasm, Lysotracker Green to visualize acidic cellular compartments (central panel), and with an antibody against the lysosomal marker LAMP-1 (right panel). The nuclei of the latter cells were also stained blue with Hoechst 33258. The first two pictures show an overlay of the DIC and red and green fluorescence, the last picture an overlay of blue, red, and green fluorescence. b) TEM images of BM-DCs that have internalized dextran sulfate/poly-L-arginine microcapsules at the indicated time intervals. Microcapsule shell: dotted arrows; membranes surrounding the microcapsules: open arrows. In the encircled area, microcapsule rupture and cytoplasmic invagination are clearly distinguishable. Lysosomes, endoplasmatic reticulum (ER), and a mitochondrion are indicated by the solid arrows.

electron microscopy, we now provide a detailed picture of the intracellular fate of polyelectrolyte microcapsules composed of dextran sulfate and poly-L-arginine. DCs actively engulf polyelectrolyte microcapsules (see the TEM images in Figure 1b and Figure 2b, broken arrows at 4 h and 12 h) as hollow disks with a dark, electron-dense wall. Following uptake, microcapsules were clearly surrounded by a bilayer membrane (Figure 2b, open arrows). Later on, the microcapsules' shell ruptured (Figure 2b, 24 h), which was possibly a result of macropinosome acidification and enzymatic degradation by lysosomal proteases. Microcapsule rupture was apparent from the invagination of cytoplasmic content inside the microcapsule core (Figure 2b, 24 h, white circle). At the location of the invagination, scattered shell debris can be clearly seen. The original microcapsule content however remained separated from this cytoplasmic infiltration by the macropinosomal membrane now surrounding both the exterior and interior of the microcapsule shell. Later, almost no intact capsules were visible (Figure 2b, 48 h). Further proof that cytoplasmic content did indeed infiltrate the capsule interior derives from the presence of both endoplasmatic reticulum (ER) and a mitochondrion inside the microcapsule core (Figure 2b, 48 h): in the close vicinity of the microcapsules, several lysosomal vesicles could be observed. These lysosomes might well contribute to macropinosome acidification by fusion of membranes, a hypothesis which was further supported by the presence of the lysosomal marker Lamp-1 in some microcapsule containing vesicles (Figure 2a).

The first prerequisite for polyelectrolyte microcapsules to be efficient antigen delivery vehicles is that encapsulated antigen is accessible for proteases, allowing it to become processed into peptides that can be presented to T cells. To visualize antigen processing into peptides, we encapsulated OVA-DQ, a fluorogenic substrate for proteases, inside the microcapsules. When OVA is in its native conformation, a strong fluorescence quenching is observed owing to excessive labeling with the BODIPY dye. Upon enzymatic degradation of OVA-DQ into single, dye-labeled peptides, quenching is relieved and the products become brightly fluorescent in the green channel.[39] As shown by confocal microscopy and flow cytometric analysis (Figure 3), OVA-DQ-loaded microcapsules emitted very low green fluorescence prior to cellular uptake (Figure 3a). However, even after a 4 h incubation period, internalized microcapsules already displayed a bright green fluorescence. At 48 h of incubation, green fluorescence became more and more diffuse and spread throughout the cell. The early processing of OVA into peptides within 4 h was somewhat surprising, given the fact that rupturing of the microcapsule shell, as observed by TEM, exclusively occurred at later time intervals ($t = 24$ h). This indicates that even before rupturing, the polyelectrolyte microcapsule shell is sufficiently porous to allow protease infiltration into the microcapsules and subsequent proteolytic processing of OVA.

Undoubtedly the most appealing part of using microparticulate antigen carriers in the 0.1–10 μm range is their capacity to enhance antigen presentation and especially to promote MHC-I-mediated cross-presentation to CD8 T cells, which is a feature that is mostly lacking when using soluble

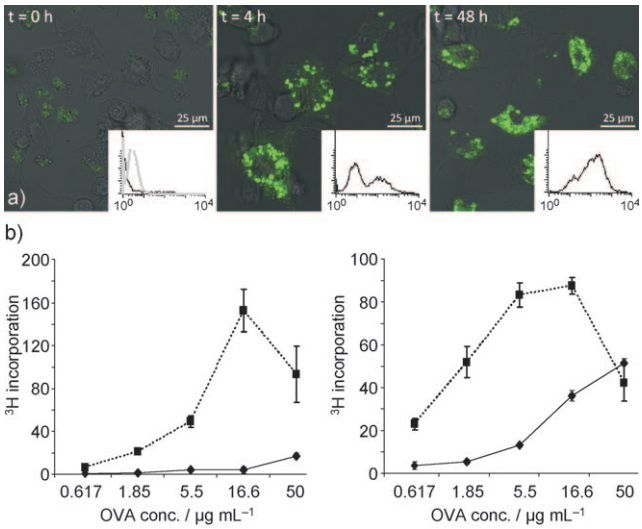

Figure 3. a) Processing of dextran sulfate/poly-L-arginine microcapsule-encapsulated OVA was analyzed using OVA-DQ. Confocal microscopy images of BM-DCs incubated with OVA-DQ microcapsules for 0, 4, and 48 h (overlay of green fluorescence and DIC). Insets: flow cytometry analysis of green fluorescence intensity (FL1-H). An overlay of DC green autofluorescence (black line) and green fluorescence intensity of OVA-DQ microcapsules (gray line) is given in the first histogram. The second and third histograms show the green fluorescence intensity after incubating BM-DCs with OVA-DQ microcapsules for 4 and 48 h, respectively. b) Antigen presentation by BM-DCs after uptake of soluble and encapsulated OVA. Proliferation of OT-I cells was used as a measure for MHC-I-mediated cross-presentation of OVA (left graph), proliferation of OT-II cells as a measure for MHC-II-mediated presentation (right). ◆, ——: OVA; ■, -----: OVA capsules.

antigens. To assess whether this also holds true for polyelectrolyte microcapsules, OVA was encapsulated as model antigen, and antigen presentation to OT-I and to OT-II T cells was assessed. OT-I cells are CD8 T cells with a transgenic T-cell receptor that specifically recognizes the OVA peptide SIINFEKL presented by MHC-I, whereas OT-II cells are transgenic CD4 T cells that specifically recognize the OVA peptide LSQAVHAAHAEINEAGR presented by MHC-II. As shown in Figure 3b, MHC-I-mediated antigen cross-presentation towards OT-I cells was dramatically increased using encapsulated OVA rather than soluble OVA; the latter allows some cross-presentation only at the highest concentration of OVA tested. In contrast, cross-presentation by microcapsule-encapsulated OVA is already significant at a 25-fold lower concentration of OVA, and it reaches a maximum at an OVA concentration of 16.6 μg mL^{-1}. At higher concentrations, the OT-I T-cell response declined, which most likely reflects cytotoxicity exerted by very high amounts of microcapsules.[22] Importantly, the increase in MHC-I-mediated presentation did not come at the expense of MHC-II-mediated presentation to CD4 T cells, which proved to be similarly elevated, especially at lower antigen concentrations (Figure 3b).

In conclusion, we have demonstrated that polyelectrolyte capsules are efficiently taken up by DCs, and the uptake involves a macropinocytotic route. Furthermore, we have unambiguously demonstrated that polyelectrolyte capsules

remain in endolysosomal vesicles, where the microcapsule shell is ruptured and encapsulated antigen is processed. Finally, we have shown that antigen-loaded polyelectrolyte capsules can efficiently stimulate CD4 and CD 8 T-cell proliferation using an in vitro antigen presentation assay. These data suggest that polyelectrolyte capsules are promising vehicles to target antigens towards DCs in vivo, which is the focus of our ongoing research.

Experimental Section

Female C57BL/6 mice for BM-DC preparation were purchased from Janvier (Le Genest Saint Isle, France), and OT-I and OT-II transgenic mice were provided by Prof. Van Kooyk from the VU University Medical Center (Amsterdam, Netherlands) and housed in a specified pathogen-free facility in micro-isolator units. At 12–16 weeks, mice were euthanized with CO_2. Bone marrow was isolated from tibia and femurs, and OT-I and OT-II cells from spleens. All mice experiments were approved by the local ethical committee.

Polyelectrolyte capsules: Calcium chloride, sodium carbonate, FITC-dextran (2000 kDa), ovalbumin (OVA; grade VII), dextran sulfate (10 kDa), poly-L-arginine hydrochloride and RITC-labeled poly-L-arginine hydrochloride (Mw > 70 kDa) were purchased from Sigma–Aldrich. OVA-DQ was purchased from Molecular Probes. $CaCO_3$ microparticles were synthesized according to Volodkin et al.[16,19] and subsequently coated by dispersing them in 5 mL of a 2 mg mL^{-1} dextran sulfate solution containing 0.5 M NaCl. Microparticles were collected by centrifugation, and residual dextran sulfate was removed by washing twice with water. Microparticles were stirred in 5 mL of a 1 mg mL^{-1} poly-L-arginine solution in 0.5 M NaCl, centrifuged, and washed again. This procedure was repeated until two bilayers of dextran sulfate/poly-L-arginine were deposited. Hollow capsules were obtained by removing the $CaCO_3$ with a 0.2 M EDTA solution (pH 5.2). Particles were washed three times and resuspended in 1 mL PBS buffer. RITC-labeled microcapsules were produced by replacing poly-L-arginine by RITC–poly-L-arginine. The capsule concentration was determined by haemocytometry to be 700 106 capsules mL^{-1}. To obtain capsules filled with OVA, 200 μL of a 5 mg mL^{-1} stock solution was added to the $CaCl_2$ solution before the addition of the Na_2CO_3 solution. Encapsulation efficiency ($51 \pm 4\%$) was determined by measuring the amount of non-encapsulated OVA using the Quick Start Bradford protein assay according to the manufacture's instructions. To prepare OVA-DQ containing microcapsules, 200 μL of 0.5 mg mL^{-1} of OVA-DQ solution was added to the $CaCl_2$ solution.

Bone-marrow-derived DCs (BM-DCs): Dendritic cells were generated using a modified Inaba protocol.[40] Bone marrow was flushed from the femurs and tibias obtained from euthanized twelve- to sixteen-week-old C57BL/6 mice. After lysis of red blood cells with ACK lysis buffer (BioWhittaker, Wakersville, MD), granulocytes and B cells were depleted using Gr-1 (Pharmingen) and B220 (Pharmingen) antibodies, respectively, and low-toxicity rabbit complement (Cedarlane Laboratories Ltd., Hornby, Ontario, Canada). Cells were seeded at a density of 2×105 cells mL^{-1} in 175 cm^2 Falcon tubes (Becton Dickinson) in DC medium (RPMI 1640 medium containing 5% LPS-free FCS, 1% penicillin/streptomycin, 1% L-glutamine, and 50 μM β-mercaptoethanol) containing 10 ng mL^{-1} IL-4 and 10 ng mL^{-1} GM-CSF (both from Peprotech, Rock Hill, NJ). After two days and again after four days of culture, the non-adherent cells were centrifuged, resuspended in fresh medium, and replated to the same Falcon tubes. On the sixth day, non-adherent cells were removed and fresh medium containing 10 ng mL^{-1} GM-CSF and 5 ng mL^{-1} IL-4 was added. On day 8 of culture, non-adherent cells were harvested and used for the experiments.

Polyelectrolyte microcapsule uptake by BM-DCs was imaged with a Leica SP5 AOBS confocal microscope. For transmission electron microscopy, cells were fixed in 4% paraformaldehyde and 2.5% glutaraldehyde in 0.1 M NaCacodylate buffer (pH 7.2) for 4 h at RT followed by fixation overnight at 4 °C. After washing three times for 20 min with buffer solution, cells were dehydrated through a graded ethanol series, including a bulk staining with 1% uranyl acetate at the 50% ethanol step followed by embedding in Spurr's resin. Ultrathin sections of a gold interference color were cut using an ultra microtome (ultracut E/Reichert-Jung), followed by a post-staining with uranyl acetate and lead citrate in a Leica ultrastainer, and collected on formvar-coated copper slot grids. They were viewed with a transmission electron microscope 1010 (JEOL, Tokyo, Japan).

Uptake and inhibitor assays: Alexa 488 Phalloidin (molecular Probes) was used to stain the actin cytoskeleton according to the manufacturer's instructions. For the inhibitor studies, cells were pretreated with Filipin III (Sigma, 10 μg mL^{-1}), chlorpromazine (Sigma, 10 μg mL^{-1}), cytochalasin D (BioSource, 10 μg mL^{-1}), and rottlerin (Calbiochem, 25 μg mL^{-1}) for 1 hour, and than incubated for 4 h with RITC-labeled polyelectrolyte microcapsules. Subsequently, cells were washed with PBS, fixed with 4% paraformaldehyde, stained with alexa 488 cholera toxin subunit B (5 μg mL^{-1}, Molecular Probes), and visualized by confocal microscopy. Nuclei were stained with Hoechst 33258.

Intracellular localization of the microcapsules was addressed by staining cells with either CellTracker Green or Lysotracker Green (both Molecular Probes) according to the manufacturer's instructions. For staining with the lysosomal marker Lamp-1, cells were fixed, permeabilized with 0.1% Triton-X100, and incubated with rabbit anti-Lamp-1 (Abcam) and alexa 488 goat anti-rabbit IgG (Molecular Probes). The degree of co-localization of microcapsules with Lamp-1 staining was determined with Volocity software as a Manders' coefficient.

Microcapsule uptake and degradation were further evaluated by electron microscopy. 105 DCs were seeded onto Teflon (Electron Microscopy Sciences) pre-treated coverslips and incubated with the polyelectrolyte microcapsules for the indicated time points. Samples were washed and fixed as described above.

To follow antigen processing of encapsulated antigens by DCs, OVA-DQ was encapsulated as described above. DCs were incubated with OVA-DQ loaded microcapsules at a 1/20 ratio (20 microcapsules/cell), and at the indicated time intervals, samples were fixed and visualized by confocal microscopy.

Cell suspensions of OVA-specific CD4 and CD8 T cells were prepared from spleen and lymph nodes from, respectively, OT-II and OT-I mice. OT-I cells are transgenic CD8 T cells with a T-cell receptor (TCR) specific for the OVA H2-Kb-restricted epitope SIINFEKL, whilst OT-II cells are transgenic CD4 T cells with a TCR specific for the OVA I-ab-restricted epitope LSQAVHAAHAEINEAGR. Single cell suspensions were prepared, and CD4 and CD8 T cells were isolated from the suspensions using Dynal mouse CD4/CD8 negative isolation kit (Invitrogen, CA, USA) according to the manufacturer.

T-cell proliferation assay: Irradiated BM-DCs were pulsed with serial dilutions of either OVA containing microcapsules or equivalent amounts of soluble OVA in a round-bottom 96-well plates and washed three times. Each concentration of soluble and encapsulated OVA was applied in triplicate onto the DCs. Microcapsules were derived from three different batches produced at the same time. Purified T cells (either CD4 T cells from OT-II mice or CD8 T cells from OT-I mice) were added to each well and co-cultured with the antigen-pulsed BM-DCs for 48 h. After 48 h, [3H] thymidine (1 μCi; Amersham Biosciences, NJ, USA) was added for 16 h to detect incorporation into the DNA of proliferating T cells. Cells were harvested onto filters and [3H] thymidine incorporation was assessed using beta counter. Graphs show a representative of three independently repeated experiments using different batches of microcapsules.

Flow cytometric analysis: All samples were measured on a FACSCalibur (BD) flow cytometer and analyzed using CellQuestTM software.

To assess processing of antigen-loaded microcapsules, DCs were incubated with OVA-loaded microcapsules and fluorescence intensity in the green channel (FL1-H) was measured by flow cytometry. Cells were gated first on the basis of a high side and forward scatter profile. Green autofluorescence of DCs and green fluorescence emitted by the OVA-DQ microcapsule suspension were measured separately.

Received: July 9, 2009
Published online: October 6, 2009

Keywords: antigens · capsules · dendritic cells · polyelectrolytes

[1] G. Ada, *N. Engl. J. Med.* **2001**, *345*, 1042.
[2] R. Rappuoli, *Nat. Biotechnol.* **2007**, *25*, 1361.
[3] R. M. Steinman, *Eur. J. Immunol.* **2007**, *37 Suppl 1*, S53.
[4] P. E. Jensen, *Nat. Immunol.* **2007**, *8*, 1041.
[5] S. T. Reddy, M. A. Swartz, J. A. Hubbell, *Trends Immunol.* **2006**, *27*, 573.
[6] K. L. Rock, L. Shen, *Immunol. Rev.* **2005**, *207*, 166.
[7] K. S. Denis-Mize, M. Dupuis, M. Singh, C. Woo, M. Ugozzoli, D. T. O'Hagan, J. J. Donnelly 3rd, G. Ott, D. M. McDonald, *Cell. Immunol.* **2003**, *225*, 12.
[8] P. Johansen, J. M. Martinez Gomez, B. Gander, *Expert Rev. Vaccines* **2007**, *6*, 471.
[9] H. Shen, A. L. Ackerman, V. Cody, A. Giodini, E. R. Hinson, P. Cresswell, R. L. Edelson, W. M. Saltzman, D. J. Hanlon, *Immunology* **2006**, *117*, 78.
[10] Y. Men, R. Audran, C. Thomasin, G. Eberl, S. Demotz, H. P. Merkle, B. Gander, G. Corradin, *Vaccine* **1999**, *17*, 1047.
[11] S. Jain, W. T. Yap, D. J. Irvine, *Biomacromolecules* **2005**, *6*, 2590.
[12] D. T. O'Hagan, M. Singh, *Expert Rev. Vaccines* **2003**, *2*, 269.
[13] D. T. O'Hagan, M. Singh, J. B. Ulmer, *Methods* **2006**, *40*, 10.
[14] G. Decher, *Science* **1997**, *277*, 1232.
[15] G. B. Sukhorukov, E. Donath, S. Davis, H. Lichtenfeld, F. Caruso, V. I. Popov, H. Mohwald, *Polym. Adv. Technol.* **1998**, *9*, 759.
[16] D. V. Volodkin, A. I. Petrov, M. Prevot, G. B. Sukhorukov, *Langmuir* **2004**, *20*, 3398.
[17] F. Caruso, R. A. Caruso, H. Mohwald, *Science* **1998**, *282*, 1111.
[18] E. Donath, G. B. Sukhorukov, F. Caruso, S. A. Davis, H. Mohwald, *Angew. Chem.* **1998**, *110*, 2323; *Angew. Chem. Int. Ed.* **1998**, *37*, 2201.
[19] D. V. Volodkin, N. I. Larionova, G. B. Sukhorukov, *Biomacromolecules* **2004**, *5*, 1962.
[20] A. I. Petrov, D. V. Volodkin, G. B. Sukhorukov, *Biotechnol. Prog.* **2005**, *21*, 918.
[21] B. G. De Geest, R. E. Vandenbroucke, A. M. Guenther, G. B. Sukhorukov, W. E. Hennink, N. N. Sanders, J. Demeester, S. C. De Smedt, *Adv. Mater.* **2006**, *18*, 1005.
[22] S. De Koker, B. G. De Geest, C. Cuvelier, L. Ferdinande, W. Deckers, W. E. Hennink, S. De Smedt, N. Mertens, *Adv. Funct. Mater.* **2007**, *17*, 3754.
[23] R. De Rose, A. N. Zelikin, A. P. R. Johnston, A. Sexton, S. F. Chong, C. Cortez, W. Mulholland, F. Caruso, S. J. Kent, *Adv. Mater.* **2008**, *20*, 4698.
[24] A. Muñoz Javier, O. Kreft, A. P. Alberola, C. Kirchner, B. Zebli, A. S. Susha, E. Horn, S. Kempter, A. G. Skirtach, A. L. Rogach, J. Radler, G. B. Sukhorukov, M. Benoit, W. J. Parak, *Small* **2006**, *2*, 394.
[25] C. Cortez, E. Tomaskovic-Crook, A. P. R. Johnston, B. Radt, S. H. Cody, A. M. Scott, E. C. Nice, J. K. Heath, F. Caruso, *Adv. Mater.* **2006**, *18*, 1998.
[26] U. Reibetanz, D. Halozan, M. Brumen, E. Donath, *Biomacromolecules* **2007**, *8*, 1927.
[27] H. Ai, J. J. Pink, X. T. Shuai, D. A. Boothman, J. M. Gao, *J. Biomed. Mater. Res. Part A* **2005**, *73*, 303.
[28] B. G. De Geest, S. De Koker, G. B. Sukhorukov, O. Kreft, W. J. Parak, A. G. Skirtach, J. Demeester, S. C. De Smedt, W. E. Hennink, *Soft Matter* **2009**, *5*, 282.
[29] A. Muñoz JavierJavier, O. Kreft, M. Semmling, S. Kempter, A. G. Skirtach, O. T. Bruns, P. del Pino, M. F. Bedard, J. Raedler, J. Kaes, C. Plank, G. B. Sukhorukov, W. J. Parak, *Adv. Mater.* **2008**, *20*, 4281.
[30] A. Lanzavecchia, *Curr. Opin. Immunol.* **1996**, *8*, 348.
[31] A. von Delwig, E. Bailey, D. M. Gibbs, J. H. Robinson, *Eur. J. Immunol.* **2002**, *32*, 3714.
[32] K. Sarkar, M. J. Kruhlak, S. L. Erlandsen, S. Shaw, *Immunology* **2005**, *116*, 513.
[33] J. E. Schnitzer, P. Oh, E. Pinney, J. Allard, *J. Cell Biol.* **1994**, *127*, 1217.
[34] P. A. Orlandi, P. H. Fishman, *J. Cell Biol.* **1998**, *141*, 905.
[35] L. H. Wang, K. G. Rothberg, R. G. W. Anderson, *J. Cell Biol.* **1993**, *123*, 1107.
[36] G. B. Sukhorukov, A. L. Rogach, B. Zebli, T. Liedl, A. G. Skirtach, K. Kohler, A. A. Antipov, N. Gaponik, A. S. Susha, M. Winterhalter, W. J. Parak, *Small* **2005**, *1*, 194.
[37] U. Reibetanz, C. Claus, E. Typlt, J. Hofmann, E. Donath, *Macromol. Biosci.* **2006**, *6*, 153.
[38] O. Kreft, A. M. Javier, G. B. Sukhorukov, W. J. Parak, *J. Mater. Chem.* **2007**, *17*, 4471.
[39] M. E. Wikstrom, E. Batanero, M. Smith, J. A. Thomas, C. von Garnier, P. G. Holt, P. A. Stumbles, *J. Immunol.* **2006**, *177*, 913.
[40] G. J. Randolph, K. Inaba, D. F. Robbiani, R. M. Steinman, W. A. Muller, *Immunity* **1999**, *11*, 753.

